

Analyzing and Predicting Anisotropic Effects of BRDFs

Jiří Filip*

Institute of Information Theory and Automation of the CAS

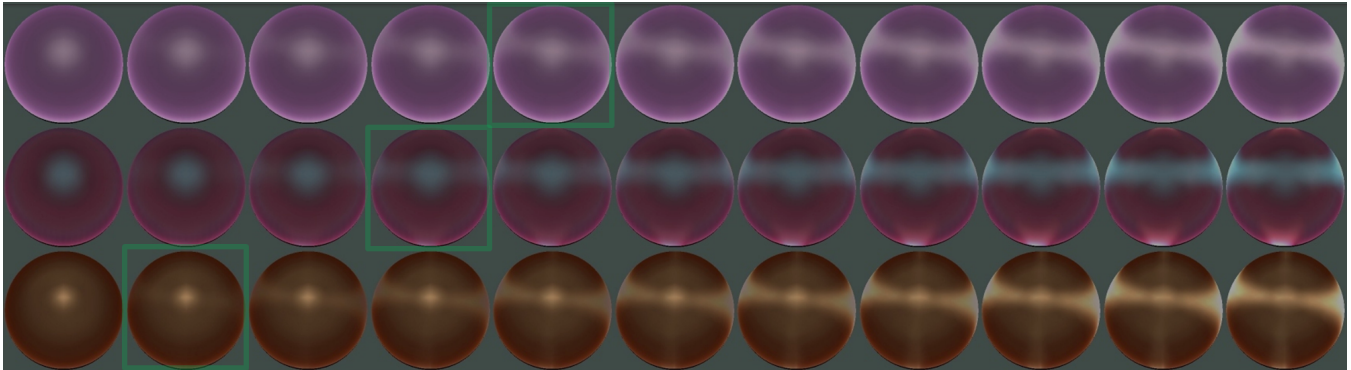


Figure 1: Example of three BRDFs on sphere having their anisotropic appearance scaled from isotropy (left) to full anisotropy (right) in ten steps. Images corresponding to threshold of perceived anisotropy estimated by the proposed anisotropy measure A_L are framed.

Abstract

The majority of the materials we encounter in the real-world have variable reflectance when rotated along a surface normal. This view and illumination azimuthally-variable behavior is known as visual anisotropy. Such behavior can be represented by a four-dimensional anisotropic BRDF that characterizes the anisotropic appearance of homogeneous materials. Unfortunately, most past research has been devoted to simplistic three dimensional isotropic BRDFs. In this paper, we analyze and categorize basic types of BRDF anisotropy, use a psychophysical study to assess at which conditions can isotropic appearance be used without loss of details in material appearance. To this end, we tested the human impression of material anisotropy on various shapes and under two illuminations. We conclude that subjects sensitivity to anisotropy declines with increasing complexity of 3D geometry and increasing uniformity of illumination environment. Finally, we derive and perceptually validate a computationally efficient measure of material visual anisotropy.

CR Categories: I.3.7 [Three-Dimensional Graphics and Realism]: Color, shading, shadowing, and texture— [J.4]: Social and Behavioral Sciences—Psychology

Keywords: anisotropy BRDF measure psychophysical user-study material appearance

1 Introduction

Anisotropic materials are, due to their atypical light-transport properties, often used in achieving an eye-catching look of many man-made products as shown in Fig. 2. Fabrics for fancy apparel are probably the most typical example; however, intrigue metallic gift

wrapping papers or greetings cards also often exhibit anisotropic behavior. The anisotropic finishing of plastics or metals is often used to create an expensive look in personal items or electronics. Genuine wooden materials are also very popular due to their specific anisotropic behavior.



Figure 2: Real-world examples of anisotropic appearance of materials: fabric, machined plastic, and polished wood. Anisotropy is caused by the orientation of different threads of fibers, parallel grooves (causing highlight perpendicular to their direction), and wooden fibers (exhibiting both specular (left) and anisotropic (right) highlights), respectively.

In general, anisotropy is the property of being directionally dependent, as opposed to isotropy, which implies identical properties in all directions. It is most often observed in chemistry and physics in evaluating a material's optical and structural properties [Wenk and Houtte 2004]. In computer vision related applications, isotropy and anisotropy are used in the analysis of directionally-dependent material's appearance and capabilities of the related methods. When material's reflectance is constant for fixed view and illumination irrespective to the rotation of the material around its normal, the material is considered isotropic. In contrast, materials whose reflectance is not constant are considered anisotropic. This also extends to measurement and modeling methods, as they can be categorized into two groups depending on their ability to measure or model anisotropic behavior.

Based on final application requirements, material appearance can be represented either by reflectance using BRDF [NICODEMUS et al. 1977], by directionally-varying texture using BTF [Dana et al. 1999] or SVBRDF, or by more complex light transport functions, e.g., BSSRDF [NICODEMUS et al. 1977]. Some of these representations can preserve most of the important visual aspects of a mate-

*e-mail: filipj@utia.cas.cz

rial appearance (e.g., shadowing, masking, inter-reflections, sub-surface scattering) albeit at the cost of high storage and acquisition. In contrast BRDF assumes homogeneous materials, i.e., omits any texture information, and is based on simplifying assumptions of opaque and flat materials. In our work, we focus on BRDF (Bidirectional Reflectance Distribution Function) [NICODEMUS et al. 1977] describing the ratio of energy reflected by the material for certain combinations of incoming and outgoing directions. When we assume separate processing of color channels, the anisotropic BRDF is a four-dimensional function $B(\theta_i, \varphi_i, \theta_v, \varphi_v)$ as shown in Fig. 3-b. The BRDF can be further reduced to a three-dimensional isotropic function by omitting material anisotropy, i.e., $B(\theta_i, \theta_v, \varphi_i - \varphi_v)$. Incoming and outgoing directions are specified by θ elevation and φ azimuthal angles. Moreover, a bilateral symmetry of BRDF [ROMEIRO et al. 2008], valid for the majority of materials, allows additional folding of azimuthal subspace into interval $(0, \pi)$ resulting in $B(\theta_i, \theta_v, |\varphi_i - \varphi_v|)$ as shown in Fig. 3-a.

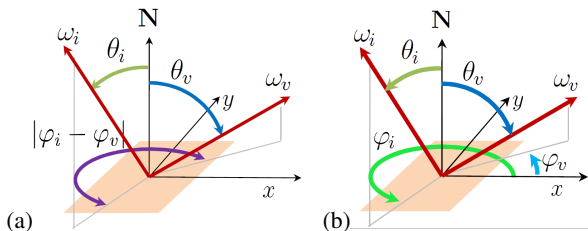


Figure 3: A comparison of (a) isotropic and (b) anisotropic BRDF parameterization.

Fig. 4 compares isotropic and anisotropic materials and their BRDFs. Note that BRDFs unfolded into 2D are, due to illumination and view reciprocity, symmetric matrices with rows and columns representing illumination and view directions circling from the pole to the bottom of the hemisphere above the described material.

Because of its inner micro-structure made from elements almost always to a certain extent directional, visual anisotropy is natural for the majority of both natural and man-made materials. However, many BRDF measurement and modeling approaches cut their processing costs by omitting anisotropic behavior; therefore our work focuses on an analysis of conditions allowing this simplification without having an impact on perceived details in a materials appearance. Although the directionally-dependent visual anisotropy of materials is a well-established notion [WARD 1992], [LU et al. 2000], to date its interaction with shape and illumination conditions relative to human perception has not been adequately studied.

Furthermore, we use an anisotropic BRDF dataset to psychophysically analyze perceptual effects of material anisotropy and propose a relevant measure of anisotropy. We ascertain that the computational analysis of perceptual anisotropic effects would be beneficial especially for making applications of material measurement, design, or visualization more efficient, yet without compromising perceived fidelity. Such Inquiry can also be used to predict whether materials exhibit anisotropic behavior and consequently in determining between isotropic or full anisotropic BRDF measurement approaches. An efficient material anisotropy measure would allow for a fast identification of the degree of anisotropy for unknown materials; therefore, enabling a designer to select an appropriate BRDF from a database, or tune accordingly parameters of anisotropic model. The proposed measure can also be utilized to evaluate the anisotropic visual effects of new surfaces at the design stage, i.e., prior to manufacturing. Another application could be material retrieval according to the required intensity or type of anisotropic behavior.

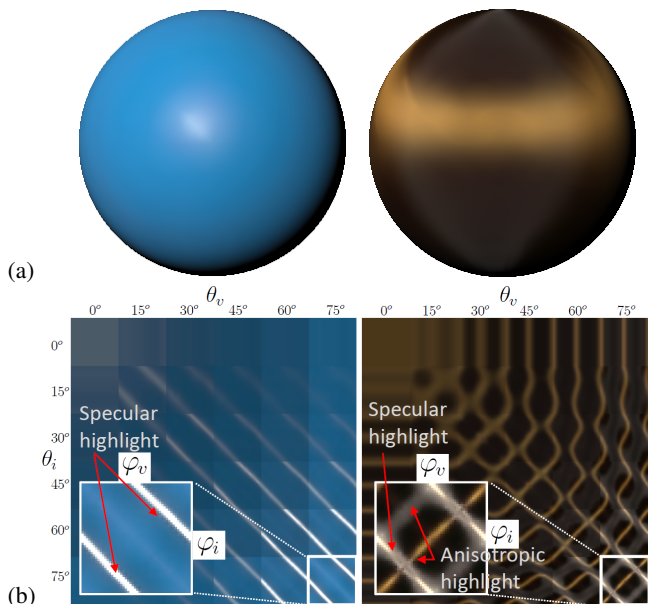


Figure 4: (a) Comparison of appearance of isotropic (left) and anisotropic (right) material rendering. (b) Their corresponding 4D BRDFs unfolded to 2D image. Each square block depicts illumination and view azimuth-dependent reflectance for fixed elevation angles (φ_i/φ_v). The blocks are ordered horizontally/vertically with increasing view/illumination elevation angle (θ_i/θ_v).

Major contributions of this paper are:

- an analysis and categorization of individual types of anisotropy we encountered
- a psychophysical analysis evaluating perceived anisotropy of over two hundreds of anisotropic BRDFs, three shapes, and two illumination conditions
- introduction of two computational measures of directionally dependent anisotropy,
- a comparison of results obtained from the psychophysical study and the proposed computational measures

The paper initially looks at anisotropy related research in Section 2, and test data in Section 3. Then, different types of material anisotropy are presented in Section 4 and the human perception of anisotropy is analyzed in Section 5. Section 6 proposes new computational measures of anisotropy relative to results of the experiment, while Section 7 concludes the paper.

2 Prior Work

Most of the work relating to anisotropy in computer vision deals with textural information. Past research studies psychophysical aspects of visual anisotropy [HANSEN et al. 2008], [ONS et al. 2011] and creates statistical models describing the relationship between perceived and computational textural anisotropy [ROLI 1996], [WENK and HOUTTE 2004], [ONS et al. 2011] or directionality [SHAH et al. 2008]. Anisotropy has been also used as a metric for image fidelity and quality assessment [GABARDA and CRISTÓBAL 2007].

To date, also several analytical BRDF models capable of representation of anisotropic reflections appeared [WARD 1992], [LAFORTUNE et al. 1997], [ASHIKHMIN and SHIRLEY 2000], [KURT et al. 2010]. They

are able to reproduce certain anisotropic effects, however, their demanding fitting requires sufficient number of directional samples and relies on setting of proper initial conditions. Therefore, fitting becomes practically intractable for more than two lobes.

Prediction of anisotropic highlights locations was already studied [Lu et al. 2000] and recently further extended to arbitrary geometry with interactive tangents editing [Raymond et al. 2014]. Simplified method of anisotropic highlight detection for purpose of anisotropic materials adaptive measurement was shown in [Filip and Vavra 2015]. Despite the research community being well aware of difficulties connected with the reproduction of directionally dependent anisotropic behavior, due to the lack of anisotropic data, there has been neither any psychophysical study evaluating to which extent the anisotropic appearance is perceptually salient, nor any computational measure that could simulate human judgment available. Initial perceptual study of BTF [Dana et al. 1999] comprising also analysis of directional anisotropy [Filip and Haindl 2012] has not been very conclusive. Apart from this, we are not aware of any research evaluating the extent of perceived anisotropy for different shapes and illuminations.

Our work analyzes perceptual effects of anisotropic behavior of spatially homogeneous materials, i.e., without texture information, based purely on their illumination- and view-dependent directional behavior represented by BRDFs. We propose and perceptually validate a computationally efficient measure of anisotropy and its easy-to-acquire approximation, that shows a high correlation with the perceived anisotropy.

3 Test Dataset

Due to its simplicity, most BRDF related research is, only focused on isotropic BRDF related materials. A comprehensive public BRDF database of isotropic measurements was introduced in [Matusik et al. 2003] and additional BRDFs in [Günther et al. 2005] and [Marschner et al. 2000]. In regard to anisotropic measurements, four detailed datasets are available [Ngan et al. 2005], three probes of fabric materials [Filip et al. 2014], and additional 150 in a recently published UTIA BRDF database [Filip and Vavra 2014]. For the purposes of this paper we used this comprehensive database, which we enlarged by including an additional 67 BRDFs obtained by the averaging of spatially-varying materials. The resulting dataset comprises 217 BRDFs and covers a wide range of reflectance behavior from samples of fabric, leather, wood, etc. to unusual materials like retro-reflective tape and lenticular card. A collection of all BRDFs and their renderings is shown in the supplementary material. The elevation angular resolution of the BRDF is 15° and azimuthal resolution is 7.5° resulting into 288 illumination \times 288 viewing directions. Although the resolution might seem rather low, we believe that it is sufficient as most of the samples do not exhibit highly specular behavior and thus the highlights are recorded correctly.

4 Categorization of Anisotropy Types

Based on types of anisotropic behavior found in our test dataset, we can roughly categorize the measured BRDFs into four basic groups. For each group we show in Fig. 5 an example of BRDF subset being a function of azimuthal angles φ_i and φ_v for fixed elevation angles $\theta_i = \theta_v = 75^\circ$ (shown in Fig. 4-b) and its rendering on a sphere.

- **Group A** – no or very faint anisotropy (given by random structure of surface features). This is the case for paint, paper, most upholstery fabric and leather materials.

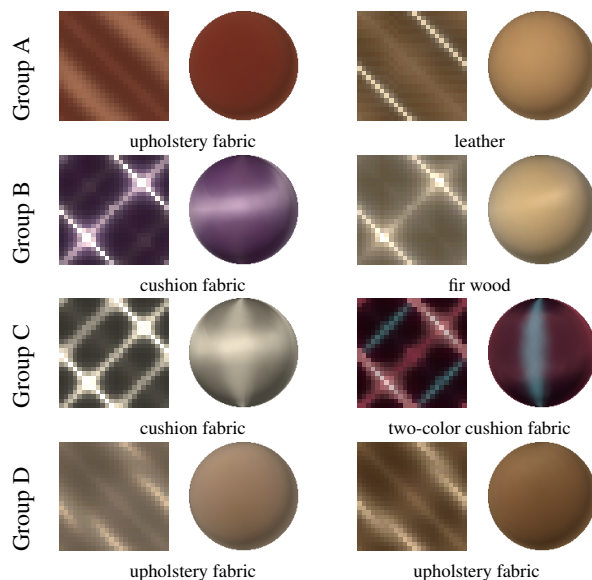


Figure 5: Examples of four anisotropy types typically present in real-world materials. BRDF subspace for elevations θ_i/θ_v (left) and its rendering on sphere (right).

- **Group B** – one anisotropic highlight of variable width (usually of color similar to specular highlight). This is the case for all measured wood samples and many fabric. All wood materials have a distinct sharp anisotropic highlight and overall, a very similar BRDF.
- **Group C** – two anisotropic highlights. This type of anisotropy appears in fabric materials consisting of threads of fibers interwoven in different directions. Based on the colors of the threads these anisotropic highlights have either the same or different colors. Their mutual overlap can reveal information about the weaving style of the fabric.
- **Group D** – These materials have only a very faint anisotropic highlight; however, they have a variable intensity/location of specular highlight. This behavior is specific for BRDFs obtained by integration over a macroscopic geometry and/or orientation of velvet-like patches in the material. While the behavior of the first three categories of materials can be reproduced by analytic BRDF models, the behavior exhibited by this group of materials cannot be recreated in this way due to an azimuthally dependent intensity and shape of specular highlights.

A distribution of materials from the tested database into individual groups, based on our subjective visual analysis of their BRDFs, is shown in the first row of Tab. 1 and in detail, in the supplementary material. The table includes for groups B,C,D the sizes of subsets exhibiting strong anisotropy.

Table 1: A distribution of the tested BRDFs into the four anisotropy categories.

group	anisotropy	normal	strong	all
A	no or very faint	44	–	44
B	one anisotropic highlight	18	26	44
C	two anisotropic highlights	20	14	34
D	variable specular highlight	92	3	95
All		174	43	217

5 Visual Perception of Anisotropy

In contrast to isotropic BRDFs, anisotropic ones require additional processing prior to perceptual analysis. Therefore, first we describe methods of anisotropic highlight alignment and computation of reference isotropic BRDFs.

5.1 Anisotropy Alignment

Contrary to analysis of isotropic BRDFs, where locations of specular highlights can be predicted, the analysis of anisotropic ones is more challenging. The number and location of anisotropic highlights in angular space is unknown and thus depends entirely on the initial orientation of the measured material and its optical properties. Although we could preserve original orientations of major anisotropy axes, the location of anisotropic highlights on the object would be arbitrary. This would impact consistency of our psychophysical study. Therefore, before different anisotropic BRDFs can be compared, first they must be aligned according to the main anisotropic axis.

We use the procedure proposed in [Filip and Vavra 2014]. It processes BRDF subspace for fixed elevation angles independently (see Fig. 6). Because the subspace is circularly symmetrical, its

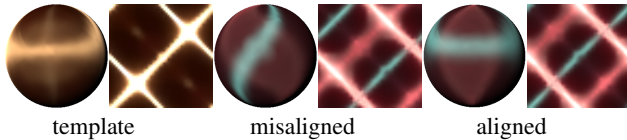


Figure 6: Example subspace anisotropy alignment using the pre-defined template.

circular shift in diagonal direction will have the same effect as the change of initial rotation of the measured sample prior to the measurement. After each shift we evaluate the distance between the shifted variant and the template represented by highly anisotropic material of the desired alignment. We select such a shift for the final alignment that produces the lowest difference from the template material.

5.2 Isotropy Enforcement

A main difference between isotropic and anisotropic BRDFs is presence of anisotropic highlights as we can see in Fig. 4. Isotropic BRDF has only specular highlights, shown as diagonal bright lines, near the angular locations where $|\varphi_i - \varphi_v| = \pi$. On the other hand, anisotropic materials exhibit highlights whose position in angular space depends on both azimuthal and elevation angles.

As we analyze perceptual importance of BRDF visual anisotropy in this paper, we need some kind of reference isotropic variant of the measured anisotropic BRDF. For this reason we propose an isotropy enforcement method that substitutes all values for fixed $|\varphi_i - \varphi_v|$ by its median value. We tested also using mean value; however, in this a case the higher intensity highlights shifted the color hue of the entire BRDF. Note that although different isotropy enforcement methods exist, they all produce isotropic BRDF with possibly different color and/or luminance shifts. Fig. 7 shows BRDFs of highly anisotropic material with its isotropy enforced variant. This approach allows us to achieve the appearance of anisotropic material as if it was represented by an isotropic BRDF model.

Although, this method does not conserve energy in BRDF by attenuation of anisotropic highlight, the results are convenient for our

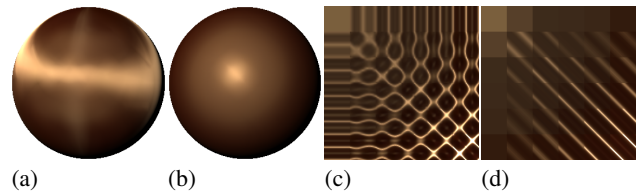


Figure 7: Rendering of an anisotropic material (a) and its version after enforcing isotropy (b). Original BRDF (c) and isotropy enforced BRDF (d).

further experiments as the color of the background and intensity of specular reflection remain the same.

5.3 A Psychophysical Experiment

The quantification of human perception of anisotropy is difficult as directionally-dependent anisotropy is not as graspable a concept for subjects as e.g., specularity or roughness. Therefore, user studies requiring subjects to evaluate anisotropy intensity on some scale tend to produce unreliable data [Filip and Haindl 2012]. To avoid this problem we reduce the problem to 2AFC decision task requiring the user to decide whether two visuals are the same or different, i.e., material is isotropic (result 0) or anisotropic (result 1).

Experimental Stimuli – Proposed is an experiment analyzing the ability of human subjects to detect anisotropic behavior of $N = 217$ BRDFs. Out of these BRDFs, 67% exhibit some sort of anisotropy. We prepared experimental stimuli consisting of two objects as shown in Fig. 8. One of them is rendered using original BRDF, while the other uses BRDF with enforced isotropy (see Sec. 5.2). Their order is random. The background of the point-light illuminated stimuli and the remaining space on the screen was set to dark gray. Note that the main axis of anisotropy has been aligned as described in Sec. 5.1. Although Vangorp et al. [2007] suggest a sphere has an inappropriate geometry for the visual comparison of BRDFs, because of its low curvature not visually masking possible differences and its overall simplicity we used it as our baseline shape. Additionally, we used a more complex blob (as recommended in [Vangorp et al. 2007]) and tablecloth shapes. For the point-light illuminated stimuli, the light was positioned slightly above the viewing direction. Tangent vectors for shapes *sphere* and *blob* correspond to parallels, while for *table* are parallel with edges of the tablecloth. Finally, we also included a sphere in the *grace*¹ illumination environment in order to assess a subjects sensitivity to anisotropy under different illuminations. The environment maps were approximated by a set of 64 discrete point-lights. We chose to test the *sphere* under different types of illumination because its geometry provides a wide range of illumination and viewing combinations without introducing the distracting effects of higher curvatures. Example stimuli images for BRDF of wood are shown in Fig. 8. All together we have four sets of stimuli each containing 217 images, i.e., a total 868 trials.

Participants and Experimental Procedure – Six volunteer subjects (author and five naive observers) performed the experiment in four sessions. All subjects had normal or corrected to normal vision and all but the author were naive with respect to the purpose and design of the experiment. Subjects had to decide whether there was any visible difference (caused by BRDF anisotropy) between the spheres or not. There was no strict time limit for answers but they were instructed to complete each stimulus image within few seconds in order to avoid a pixel-wise comparison. All stimuli were presented on a calibrated 24" HP LP2475w display (60Hz, resolution 1920×1200, color temperature 6500K, gamma 2.2, luminance

¹<http://www.debevec.org>

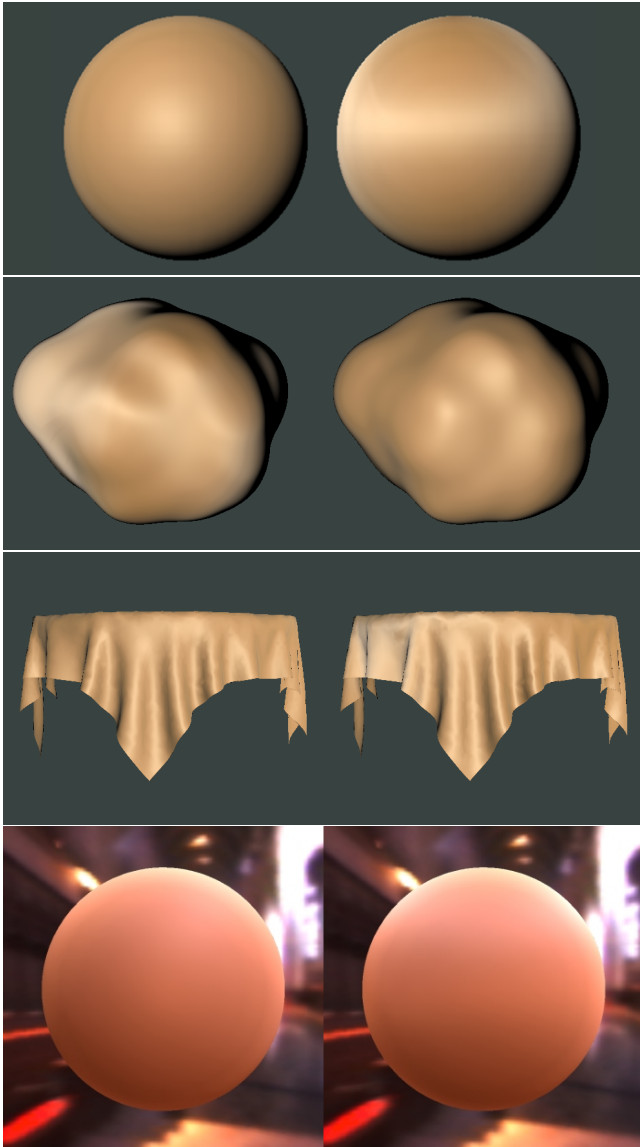


Figure 8: Example of stimuli images for material wood and all three shapes tested (sphere, blob, table) and illuminations (point-light, grace) used in four sessions of our psychophysical study.

120 cd/m²) under dim room environment. Participants viewed the screen at a distance of 0.5m, so that each object in a pair subtended an approximately 12° of visual angle. There was a pause of 0.5 s between stimuli presentations, and, over four sessions, participants took on average 40 minutes to perform the whole experiment.

In complement to the controlled study, we also performed a web-based experiment with the goal to validate the reliability of conclusions by a greater number of subjects. In total, 27 subjects performed a session with the sphere illuminated by a point light. A correlation between averaged results of the controlled and web-based studies was 0.8777 ($p_{val}=0.00001$), therefore supporting the consistency of results obtained in the controlled experiment.

Results – The averaged binary responses of all six subjects are shown in Fig. 12. As expected, the obtained perceived anisotropy is, due to a binary decision task, often saturated. Similarly, on a psychophysical note, we used 50% as a threshold of notice-

able anisotropy (i.e., $t_E = 0.5$ shown as a red line in Fig. 12), i.e., 50% of subjects identified the difference between the isotropic and anisotropic sphere. Fig. 9 shows a total of n_E materials that were above this threshold and thus are considered as perceptually anisotropic in individual sessions. In the first three bars we observed a decreasing sensitivity of subjects in accordance with the increasing complexity of rendered objects. The complexity of the objects approximated by a standard deviation of difference of their normalized vertices from the object’s center of gravity σ_V is shown in the second column of Fig. 10. The second column provides durations of trials in individual experiment sessions averaged across all BRDFs and subjects. It depicts increasing difficulty in identifying anisotropy with greater scene complexity.

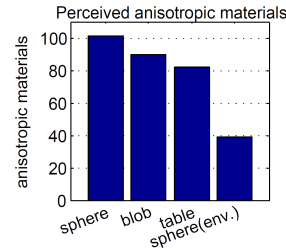


Figure 9: Overall number of perceived anisotropic materials across different shapes and illuminations.

Figure 10: Tested shapes curvature approximated by a standard deviation of difference of its vertices from the object’s center of gravity.

An even more significant drop of perceptual sensitivity to anisotropy was observed when environment illumination was used instead of a point-light (see last bar of Fig. 9). This suggests the more uniform the illumination, the less important is the perceived anisotropy of an illuminated surface.

Finally, Fig. 11 shows subjects responses for individual categories of anisotropy as a function of (a) shapes and (b) illumination type. One can see that these results follow the observations above. The only exception in Fig. 11-a is an increased number of responses for the shape *table* in groups A and C. As this shape is the most complex of all tested, we assume that its high curvature afforded to subjects a wider range of illumination and view directions and thus allowed for an easier distinguishing of BRDFs with two faint anisotropic highlights (group C) than in the case of a more simplified *blob* surface. All types of anisotropy mark an approximately two-thirds decrease of perceived sensitivity when the *grace* illumination environment was used (see Fig. 11-b).

5.4 Discussion

Our results show, similar to conclusions of Kozlowski et al. [2007], that more complicated shapes (with a sufficiently complicated second derivative) effectively mask the visibility of BRDF rendering imperfections. In our case, the imperfections can translate into a shift from anisotropic to isotropic materials. We conclude, again in accordance with [Kozlowski and Kautz 2007], that anisotropy is less apparent for more diffuse illuminations. We assume the more uniform the illumination, the less apparent the anisotropic behavior of the illuminated surface. Thus, illumination representing several bright light sources will allow for an easier detection of anisotropy than many equally distributed lights of a similar intensity. Note that our conclusions are based on static stimuli, and we assume that for dynamic stimuli the anisotropic appearance will become more apparent. More details on subjects’ performance over different shapes and on strong anisotropic materials only are shown in the supplementary material.

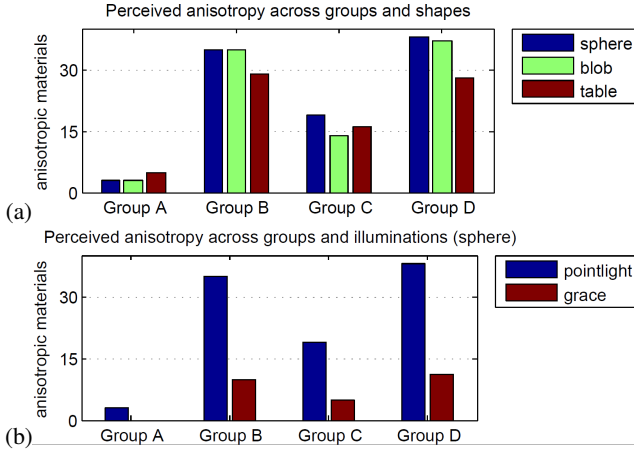


Figure 11: Results of the controlled psychophysical study – overall number of perceived anisotropic materials across different shapes and illuminations, distributed into four types of anisotropy as a function of shape (a), and illumination (b).

6 Proposed Anisotropy Measures

Our goal is to develop a perceptually related measure of visual anisotropy. As the principle of anisotropy detection lies in capturing differences in reflectance for fixed illumination and view directions with regard to the rotation of a material sample around its normal, we derive our measure similarly.

6.1 Global Anisotropy Measure

First we define a vector of reflectance values $\mathbf{V}_{\theta_i, \theta_v, \alpha}$ recorded during sample rotations around its normal, where θ_i and θ_v are illumination and view elevation angles, and $\alpha = |\varphi_i - \varphi_v|$ is the difference between illumination and view azimuthal angles. Let $m_{\theta_i, \theta_v, \alpha}$ be a median value of $\mathbf{V}_{\theta_i, \theta_v, \alpha}$. Note that, if values in the vector \mathbf{V} are substituted by its median value m for all combinations of $\theta_i, \theta_v, \alpha$, an isotropic enforced variant of the material is obtained and used for stimuli preparation. Using median instead of mean value avoids increasing overall material brightness, by the contribution of values along anisotropic highlights.

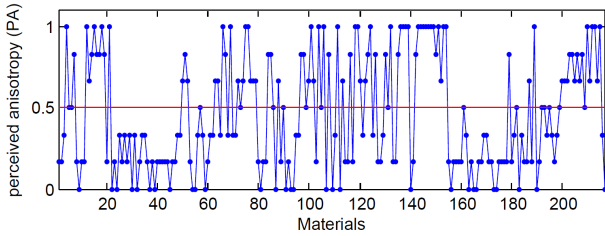


Figure 12: Results of the estimated perceived anisotropy based on user study across all tested materials rendered on sphere.

Finally, the anisotropy measure is defined as the mean average difference between vector \mathbf{V} and its median value m as

$$A = \frac{1}{C|\theta_i||\theta_v||\alpha|} \sum_{i=1}^3 w_i \sum_{\theta_i=0}^{\pi/2} \sum_{\theta_v=0}^{\pi/2} \sum_{\alpha=0}^{2\pi} |\mathbf{V}_{\theta_i, \theta_v, \alpha} - m_{\theta_i, \theta_v, \alpha}|, \quad (1)$$

where $w = [0.213, 0.723, 0.072]$ are RGB perceptual weights, and C is the normalization coefficient representing the mean BRDF

value. The normalization by C allows comparable measure responses regardless the BRDFs of different dynamic range.

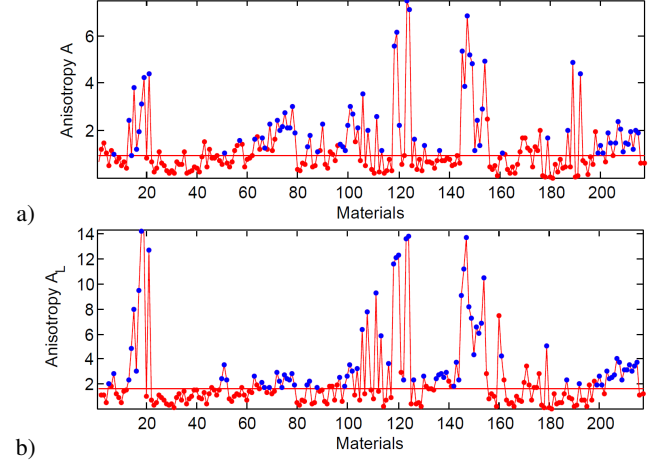


Figure 13: Results of the proposed anisotropy measure computed (a) from entire BRDF data A , (b) from a single BRDF slice A_{1S} . The blue dots marks the BRDFs identified as anisotropic in the experiment (sphere under point-light).

Results of the proposed measure (1) computed across all materials are shown in Fig. 13-(a). Note that (1) gives equal weight to each BRDF sample, and thus implements an integration weighted by $\cos \theta_i \cdot \cos \theta_v$. Although other sampling methods can be used, they were not tested.

6.2 Approximate Local Anisotropy Measure

The global measure A computes anisotropy using the entire BRDF data; however, such information is rarely available for an unknown material. Hence, its approximation using a very limited, and easy to measure, BRDF subset is needed. Similarly, to measure A we compute the difference between reflectance and its median value, for a single combination of angles $\theta_i, \theta_v, \alpha$. Although one can select arbitrary combination of elevation angles we use $\theta_i = 75^\circ, \theta_v = 75^\circ, \alpha = 15^\circ$, because the anisotropic behavior is most distinct for grazing angles and small difference between illumination and viewing azimuths. The approximate measure A_S is defined as

$$A_L = \frac{1}{C_L} \sum_{i=1}^3 w_i |\mathbf{V}_{\theta_i, \theta_v, \alpha} - m_{\theta_i, \theta_v, \alpha}|, \quad (2)$$

where w are the RGB perceptual weights and C_L is the normalization coefficient representing the mean measured reflectance value. Results of the A_L measure (2) computed across all materials as shown in Fig. 13-(b) illustrate reasonable likeness to the global measure A . The findings of both proposed measures A and A_L have a very high mutual correlation across all materials $\rho_{A-A_L} = 0.81$.

6.3 Perceptual Validation of the Measures

This section compares results of the proposed measures with those of the psychophysical experiment. For the sake of automatic material's anisotropy analysis, the human subjects ought to be substituted by the proposed computational measure. Similarly, for the experimental data threshold t_E , it is necessary to find the corresponding threshold that defines whether the material is considered anisotropic or not. Therefore, we suggest deriving this computational threshold t_M as a median value of the anisotropy measure

across all materials from our dataset. We obtained value $t_m = 0.97$ for measure A and $t_m = 1.66$ for measure A_L shown as a red horizontal outlines in Fig. 13-a,b. Although, these values are based on a limited collection of material behavior represented by our BRDF dataset, we believe that since it covers a wide variability of possible angularly-dependent behavior. Therefore, we do not expect this value would vary too much with the inclusion of additional BRDFs. Materials identified as anisotropic by both the experiment and computational measures are marked by blue dots in Fig. 13.

Using the threshold t_m , we estimate the number of anisotropic materials n_m , and given the intersection with psychophysically labeled anisotropic materials $n_i = n_e \cap n_m$, we can compute precision P and recall R retrieval rates

$$P = \frac{N_C}{N_C + N_F} = \frac{n_i}{n_m} \quad R = \frac{N_C}{N_C + N_M} = \frac{n_i}{n_e}, \quad (3)$$

where N_C, N_M, N_F are numbers of correctly detected, missed, and falsely detected anisotropic materials, respectively. Overall correlations of the measures with data of the psychophysical study as well as retrieval results are shown for individual types of anisotropy in Fig. 14. We observe the drop of precision P with increasing object complexity (Fig. 14-b). This drop is even more significant for environment illumination, while correlation with the psychophysical data and recall R rates are the highest here (Fig. 14-a,c). This implies that with the increasing complexity of shape and illumination, our measures tend to generate increasing numbers of false-positive matches, while the number of false-negatives decreases. In other words, our measures detect successfully the majority of anisotropic BRDFs identified in the psychophysical experiment; however, it overestimates perceived anisotropy with the increasing complexity of shape/illumination.

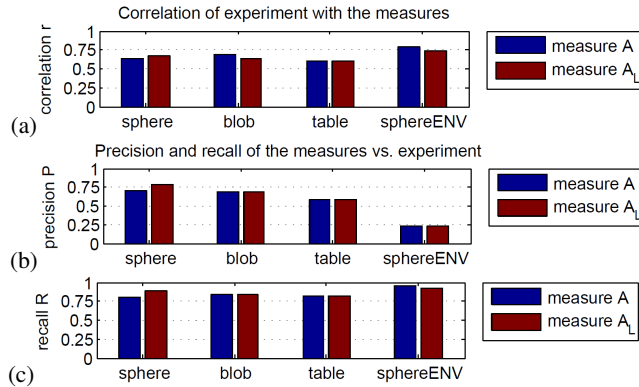


Figure 14: Performance assessment of the proposed measures: (a) correlation with the results of the psychophysical study, (b) precision P , and (c) recall R rates.

Fig. 15 compares numbers of BRDFs denoted as anisotropic by the psychophysical study with their prediction using the proposed global (A) and approximative (A_L) metrics across different categories of anisotropy (described in Section 4). The psychophysical results are averaged across all shapes and illuminations. One can observe that our measures are reasonably good especially for groups exhibiting distinct anisotropic highlights (groups B and C). On the other hand, detection of less visually apparent anisotropy caused very faint anisotropy (group A) or by integration over rough surface structures (group D), is less accurate as it tends to introduce false positive matches.

Finally, we evaluate performance of the proposed anisotropy measures over five materials having their anisotropy scaled from isotropy to full anisotropy in ten steps as shown in Fig. 1. We

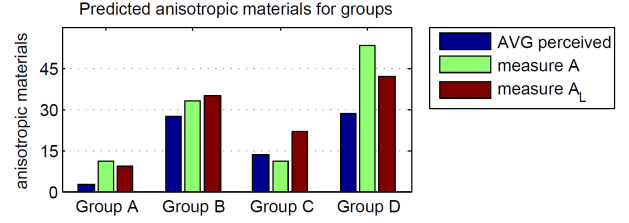


Figure 15: A comparison between results of the psychophysical study and proposed global (A) and approximative (A_L) measures, showing overall number materials indicated by anisotropic by both the study (the blue bars) and the measures.

used method similar to isotropy enforcement. Images the closest to the predicted perceived anisotropy A_L are denoted by green frame. More examples with numerical values are shown in a supplemental material.

6.4 Discussion and Limitations

The proposed approximative measure has several advantages. The first of them is computational speed which is 0.6 ms per single BRDF, while for the global measure it is 0.3 s. The second advantage is the convenient measurement of samples needed for anisotropy evaluation; because it only requires either the rotation of a mutually fixed light and camera around the sample, or rotation of the sample below the light and camera. In other words, the required values can be obtained practically by scanning unknown material using a camera with attached light rotating full circle around a material's surface normal. Therefore, no lengthy BRDF measurement is required to assess the degree of a material's anisotropy.

Deviation between the results of the psychophysical experiment and the measures can be caused by shapes used in stimuli showing just a subset of all BRDF directions. The A_L measure could potentially fail for unlikely materials exhibiting anisotropy only at lower elevation angles.

Although we have not encountered material with more than two anisotropic highlights, we believe that in general the proposed metric would work. The performance on materials having two anisotropic highlights (group C) is encouraging as shown in Fig. 15. Consistent with human perception (see examples in group C), if more anisotropic highlights are present in a single material, the measure reflects the weighted contribution of both anisotropic directions. The measure thus integrates the contribution of all anisotropic directions; therefore, its result is the same for a material with a single anisotropic highlight as for a material with two twice weaker anisotropy highlights. The proposed measure was applied to entire an BRDF where the distribution of different elevation angles was uniform. However, this is a rare case due to the variable distribution of surface elevations on the 3D object's geometry and its orientation to light and/or observer. As a future improvement, we see weighting measures' responses according to the known distribution of illumination and viewing directions present in the specific rendering of a 3D object, i.e., for a given illumination and viewing directions.

7 Conclusions

This paper presents the first perceptual analysis of a material's anisotropy as based purely on directional behavior, i.e., without textural information. First we categorized BRDFs into four main groups based on types of anisotropy. Then we ran a psychophysical study with 6 subjects analyzing the perceptual anisotropy of

217 materials represented by anisotropic BRDFs. We studied three different shapes and two illuminations, and successfully validated our results for a baseline shape by means of a web-based study over another 27 subjects.

With increasing shape complexity, we observed a decrease in subjects' sensitivity to perceived anisotropy detection. This decline was even more apparent when environment illumination was used instead of a point-light. This implies that scene and illumination complexity effectively visually masks perceived BRDF anisotropy. In other words, a simplistic isotropic appearance can be more safely used in static scenes containing complex meshes lit by a homogeneous illumination environment.

Next, we proposed two anisotropy measures; while the first one is based on entire BRDF information, the second one requires only a sparse subset of reflectance values. Both measures have a similar performance on the tested dataset, and we have shown a positive correlation with results of the psychophysical study. For each measure, we also have suggested the computational threshold approximating the psychophysical results. The achieved results demonstrate that the proposed anisotropy measures can be considered as a promising approximation of human perception of real-world visual anisotropy.

In future we plan to extend our analysis towards interactions between angularly-dependent and texturally-dependent types of anisotropy. Additionally, we would like to analyze the perception of anisotropic appearance in dynamic lighting and viewing environments.

Acknowledgments

We would like to thank all volunteers taking part in the psychophysical experiment. This research has been supported by the Czech Science Foundation grant 14-02652S and 14-10911S.

References

- ASHIKHMIN, M., AND SHIRLEY, P. 2000. An anisotropic phong light reflection model. *Journal of Graphics Tools* 5, 2, 25–32.
- DANA, K., VAN GINNEKEN, B., NAYAR, S., AND KOENDERINK, J. 1999. Reflectance and texture of real-world surfaces. *ACM Transactions on Graphics* 18, 1, 1–34.
- FILIP, J., AND HAINDL, M. 2012. User study of viewing and illumination dependent material appearance. In *In proceedings of Predicting Perceptions 2012*, 34–38.
- FILIP, J., AND VAVRA, R. 2014. Template-based sampling of anisotropic BRDFs. *Computer Graphics Forum* 33, 7 (October), 91–99.
- FILIP, J., AND VAVRA, R. 2015. Anisotropic materials appearance analysis using ellipsoidal mirror. In *IS&T/SPIE Conference on Measuring, Modeling, and Reproducing Material Appearance, paper 9398-25*.
- FILIP, J., VAVRA, R., AND HAVLICEK, M. 2014. Effective acquisition of dense anisotropic BRDF. In *Proceedings of the 22th International Conference on Pattern Recognition, ICPR 2014*, 2047–2052.
- GABARDA, S., AND CRISTÓBAL, G. 2007. Blind image quality assessment through anisotropy. *JOSA A* 24, 12, B42–B51.
- GÜNTHER, J., CHEN, T., GOESELE, M., WALD, I., AND SEIDEL, H.-P. 2005. Efficient acquisition and realistic rendering of car paint. In *Proceedings of 10th Workshop - Vision, Modeling, and Visualization (VMV) 2005*.
- HANSEN, B. C., HAUN, A. M., AND ESSOCK, E. A. 2008. The horizontal effect: A perceptual anisotropy in visual processing of naturalistic broadband stimuli. In *Visual Cortex: New Research*. Nova Science Publishers, Inc.
- KOZŁOWSKI, O., AND KAUTZ, J. 2007. Is accurate occlusion of glossy reflections necessary? In *Proceedings of the 4th symposium on Applied perception in graphics and visualization*, ACM, 91–98.
- KURT, M., SZIRMAY-KALOS, L., AND KŘIVÁNEK, J. 2010. An anisotropic BRDF model for fitting and Monte Carlo rendering. *SIGGRAPH Comput. Graph.* 44 (February), 3:1–3:15.
- LAFORTUNE, E. P., FOO, S. C., TORRANCE, K. E., AND GREENBERG, D. P. 1997. Non-linear approximation of reflectance functions. *Computer Graphics* 31, Annual Conference Series, 117–126.
- LU, R., KOENDERINK, J. J., AND KAPPERS, A. M. 2000. Singularities on surfaces with tangential hairs or grooves. *Computer Vision and Image Understanding* 78, 3, 320–335.
- MARSCHNER, S. R., WESTIN, S. H., LAFORTUNE, E. P. F., AND TORRANCE, K. E. 2000. Image-based bidirectional reflectance distribution function measurement. *Appl. Opt.* 39, 16 (Jun), 2592–2600.
- MATUSIK, W., PFISTER, H., BRAND, M., AND McMILLAN, L. 2003. A data-driven reflectance model. *ACM Transactions on Graphics* 22, 3, 759–769.
- NGAN, A., DURAND, F., AND MATUSIK, W. 2005. Experimental analysis of BRDF models. *Eurographics Symposium on Rendering 2005* 2, 117–126.
- NICODEMUS, F., RICHMOND, J., HSIA, J., GINSBURG, I., AND LIMPERS, T. 1977. Geometrical considerations and nomenclature for reflectance. *NBS Monograph 160, National Bureau of Standards, U.S. Dept. of Com.*, 1–52.
- ONS, B., VERSTRAELEN, L., AND WAGEMANS, J. 2011. A computational model of visual anisotropy. *PLoS ONE* 6, 6, e21091.
- RAYMOND, B., GUENNEBAUD, G., BARLA, P., PACANOWSKI, R., AND GRANIER, X. 2014. Optimizing BRDF orientations for the manipulation of anisotropic highlights. In *Computer Graphics Forum*, vol. 33, Wiley Online Library, 313–321.
- ROLI, F. 1996. Measure of texture anisotropy for crack detection on textured surfaces. *Electronics Letters* 32, 14 (Jul), 1274–1275.
- ROMEIRO, F., VASILYEV, Y., AND ZICKLER, T. 2008. Passive reflectometry. In *Proceedings of the 10th European Conference on Computer Vision: Part IV, ECCV '08*, 859–872.
- SHAH, P., PADILLA, S., GREEN, P., AND CHANTLER, M. 2008. Perceived directionality of $1/f^\beta$ noise surfaces. In *APGV 2008*, 203.
- VANGORP, P., LAURIJSSSEN, J., AND DUTRE, P. 2007. The influence of shape on the perception of material reflectance. *ACM Transactions on Graphics* 26, 3, 77:1–77:10.
- WARD, G. 1992. Measuring and modeling anisotropic reflection. *Computer Graphics* 26, 2 (July), 265 – 272.
- WENK, H.-R., AND HOUTTE, P. V. 2004. Texture and anisotropy. *Reports on Progress in Physics* 67, 8, 1367.